Hindawi
Advances in Condensed Matter Physics
Volume 2020, Article ID 5818403, 6 pages
https://doi.org/10.1155/2020/5818403

Research Article

Graphene-Substrate Effects on Characteristics of Weak-Coupling Bound Magnetopolaron

Zhao-Hua Ding, Yan-Bo Geng, Ying Zhao, Yong Sun, and Jing-Lin Xiao

Institute of Condensed Matter Physics, Inner Mongolia University for Nationalites, Tongliao 028043, China

Correspondence should be addressed to Zhao-Hua Ding; dzhaohua@126.com and Yong Sun; sy19851009@126.com

Received 20 December 2019; Revised 5 April 2020; Accepted 21 April 2020; Published 17 May 2020

Academic Editor: Charles Rosenblatt

Graphene has many unique properties which have made it a hotbed of scientific research in recent years. However, it is not expected intuitively that the strong effects of the substrate and Coulomb doping in the center of crystal cell on the polaron in monolayer graphene. Here, the interaction energy of surface electron (hole) in the graphene and optical phonons in the substrate, which give rise to weakly coupled polarons, is analyzed in the context of the Coulomb doping. The ground-state energy of the polaron is calculated using the Lee-Low-Pine unitary transformation and linear combination operator method. It is found that the ground-state energy is an increasing function of magnetic field strength, the bound Coulomb potential, and the cutoff wavenumber. Numerical results also reveal that the ground-state energy reduces as the distance between the graphene and the substrate is increased. Moreover, the ground energy level of polaron shows the two (+) and (−) branches and zero-Landau energy (ground) level separation in the graphene-substrate material.

1. Introduction

Monolayer graphene (MG) is the archetypal example of a zero-energy gap semiconductor. The effective mass of charge carriers near the Dirac point, a phenomenon characterized by linearly dispersive band structure, is zero. Because of its unique two-dimensional structure, graphene has a wealth of novel mechanical, thermal, optical, and electrical properties. Graphene materials have extraordinary electrical conductivity, magnitudes of order stronger than steel, and excellent optical transmission, making it widely used in high-performance nanoelectronic devices, composites, field emission materials, gas sensing, and energy storage. It is expected to replace silicon as an important raw material for the next generation of semiconductor materials. As such, graphene has been an area of intense focus in solid-state research in recent years [1–10, 15].

Studies have shown that polarons in graphene have a significant effect on the photoelectric and transport properties. Using linear combination operators and the LLP unitary transformation, Li et al. [11–13] found a regulatory mechanism of zero-Landau level splitting and that a band gap opens as a direct result of polarons. Xiao et al. [14–16] discussed the effects of Coulomb impurities and polar substrates on the splitting of polaron zero-Landau level in graphene. Wang et al. [17–21] used the LLP unitary transformation to analyse the effect of impurities on monolayer graphene's physical properties. Additionally, they calculated the effect of polarons in MG on different substrates, thereby highlighting MG's sensitivity to its local environment. Other studies [22–24] have used Huybrechts' linear combination operator and Pekar's variational approach to study magnetopolarons in MG under strong interactions between electrons and surface acoustic (SA) phonons. Despite the high interest in this area, there have been few studies on the properties of weakly coupled polarons in MG.

In this paper, the linear combination operator method and quadratic LLP unitary transformation are used to study substrate effects on the properties of bound magnetopolarons in MG under weak coupling of electrons and surface optical (SO) phonons.

2. Theory

Here, we consider MG on a substrate with the opposing side exposed to air. A uniform magnetic field is applied perpendicularly to the graphene's surface, and a bound potential created by the disordered arrangement of Coulomb impurities between the substrate and graphene is incorporated.

The Hamiltonian of such a system as shown in Figure 1, accounting for electron-SO phonon interactions can be written as

$$H = H_e + H_{ph} + H_{e-ph} - \frac{g}{r}, \quad (1)$$

where

$$H_e = V_F \begin{pmatrix} 0 & \pi_x - i\pi_y \\ \pi_x + i\pi_y & 0 \end{pmatrix}, \quad (2)$$

$$\begin{aligned} \pi_x &= \left(p_x - \frac{eBy}{2}\right), \\ \pi_y &= \left(p_y + \frac{eBx}{2}\right), \end{aligned} \quad (3)$$

$$H_{ph} = \sum_{k,v} \hbar\omega_{so,v} a_k^+ a_k, \quad (4)$$

$$\begin{aligned} H_{e-ph} &= \sum_{k,v} M_{k,v} (a_{-k}^+ + a_k) e^{ik\cdot r}, \\ M_{k,v} &= \left[\frac{\left(Q^2 \eta \hbar\omega_{so,v}\right)}{(2\varepsilon_0 k)}\right]^{(1/2)} e^{-kz}, \end{aligned} \quad (5)$$

where Q is the charge of the electron, $\eta = (k_0 - k_\infty)/[(k_\infty + 1)(k_0 + 1)]$ represents the dielectric constant of the substrate, k_∞ and k_0 are the high- and low-frequency dielectric constants, respectively, ε_0 is the frequency of phonons,$\omega_{so,v}$ is the *SO* frequency of phonons and $v = 1, 2, -(g/r)$ is the Coulomb potential, and g is the parameter of Coulomb potential which stands the strength of affecting the polaron.

One can write the momentum and position of an electron using linear combination operators [16] given by

$$\begin{aligned} p_j &= \left(\frac{\hbar\lambda}{\sqrt{2}}\right)\left(b_j^+ + b_j\right), \\ r_j &= \left(\frac{i}{\sqrt{2}\lambda}\right)\left(b_j - b_j^+\right), \end{aligned} \quad (6)$$

where $\lambda = \sqrt{eB/2\hbar}$ is the variational parameter and $j = x, y$.A Fourier series expansion is carried out to obtain the binding potential of the last term in equation (1):

$$\frac{1}{\mathbf{r}} = \frac{2\pi}{A} \sum_k \frac{1}{k} \exp(-i\mathbf{k}\cdot\mathbf{r}), \quad (7)$$

where A represents the area of graphene. The linear combination operators, equation (6), are substituted into equation (1), and the following LLP unitary transformation is performed:

$$\begin{aligned} U_1 &= \exp\left(-i\sum_k k \cdot r a_k^+ a_k\right), \\ U_2 &= \exp\left(\sum_k f_k a_k^+ - f_k^* a_k\right). \end{aligned} \quad (8)$$

Following this transformation, the result of equation (1) can be rewritten as

$$\begin{aligned} H' &= U_2^{-1} U_1^{-1} H U_1 U_2 \\ &= V_F \begin{Bmatrix} 0 & \begin{matrix} (\hbar\lambda/\sqrt{2})(b_x^+ + b_x) - \sum_k \hbar k_x (a_k^+ + f_k^*)(a_k + f_k) \\ -(ieB/\sqrt{2}\lambda)\left(b_y - b_y^+\right)/2 - (i\hbar\lambda/\sqrt{2})(b_x^+ + b_x) \\ +i\sum_k \hbar k_y (a_k^+ + f_k^*)(a_k + f_k) - ieB/\sqrt{2}\lambda(b_x - b_x^+)/2 \end{matrix} \\ \begin{matrix} (\hbar\lambda/\sqrt{2})(b_x^+ + b_x) - (eB/\sqrt{8}\lambda)(b_x - b_x^+) \\ -\sum_k \hbar k_x (a_k^+ + f_k^*)(a_k + f_k) - \left(\frac{i\hbar\lambda}{\sqrt{2}}\right)\left(b_y^+ + b_y\right) \\ -i\sum_k \hbar k_y (a_k^+ + f_k^*)(a_k + f_k) - \left(\frac{ieB}{\sqrt{8}\lambda}\right)\left(b_y - b_y^+\right) \end{matrix} & 0 \end{Bmatrix} \\ &+ \sum_{k,v} \hbar\omega_{so,v}(a_k^+ a_k + a_k^+ f_k + f_k^* a_k + f_k^* f_k) + \sum_{k,v} M_{k,v}^* (a_k^+ + f_k^+) \exp\left(-\frac{k^2}{4\lambda}\right) \exp\left(-\frac{\sum_j k_j b_j^+}{\sqrt{2}\lambda}\right) \exp\left(\frac{\sum_j k_j b_j}{\sqrt{2}\lambda}\right) \\ &+ \sum_{k,v} M_{k,v}(a_k + f_k) \exp\left(-\frac{k^2}{4\lambda}\right) \exp\left(\frac{\sum_j k_j b_j^+}{\sqrt{2}\lambda}\right) \exp\left(-\frac{\sum_j k_j b_j}{\sqrt{2}\lambda}\right) - g\frac{2\pi}{A} \sum_k \frac{1}{k} \exp\left(\sum_j \frac{k_j b_j}{\sqrt{2}\lambda}\right)\left(\exp - \sum_j \frac{k_j b_j^+}{\sqrt{2}\lambda}\right) \exp\left(-\frac{k^2}{2\lambda^2}\right). \end{aligned} \quad (9)$$

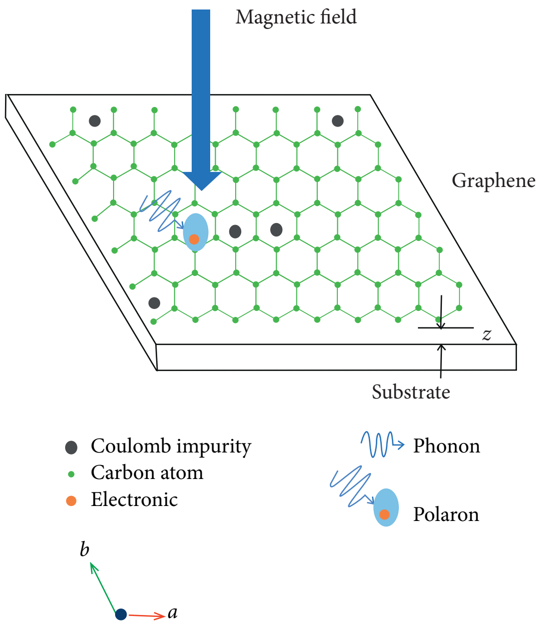

FIGURE 1: Schematic diagram of magnetopolaron in graphene with Coulomb impurities under the substrate.

Taking the wave function of the system as

$$\begin{aligned} |\psi_n\rangle\,|0\rangle &= \frac{1}{\sqrt{2}}\left(C_n'\,|n-1\rangle\,|0\rangle C_n\,|n\rangle\,|0\rangle\right), \\ C_n' &= 1-\delta_{n,0}, \\ C_n &= \sqrt{1+\delta_{n,0}}, \\ b_j^{+}\,|n\rangle &= \sqrt{n+1}\,|n+1\rangle, \\ b_j\,|n\rangle &= \sqrt{n}\,|n-1\rangle, \end{aligned} \tag{10}$$

$|0\rangle$ is the unperturbed zero-phonon state satisfying the operation $a_k\,|0\rangle = 0$.

It is straightforward to show that the expected value of the polaron subsystem is

$$\begin{aligned} E_{e,n}^2 &= \langle 0\,|\,\psi_n\,|\,H_e'^2\,|\,\psi_n\,|\,0\rangle \\ &= \frac{1}{2}V_F^2\left\{C_n'^2\sum_k \hbar^2k^2 f_k^* f_k + C_n^2\sum_k \hbar^2k^2 f_k^* f_k\right\}. \end{aligned} \tag{11}$$

The resultant eigenvalue of the electronic kinetic energy term corresponding to the zero-Landau level can be written as

$$E_{e,0} = \pm\sqrt{E_{e,n}^2} = \beta V_F \sum_k \hbar k f_k^* f_k, \tag{12}$$

where $\beta = \pm 1$. The above formula corresponds to the band exponent of the conduction band and the valence band.

In the same way, the phonon energy, electron-phonon interaction energy, and Coulomb potential energy eigenvalues for the zero-Landau level are given by

$$E_{ph,0} = \beta \sum_{k,v} \hbar\omega_{so,v} f_k^* f_k, \tag{13}$$

$$E_{e-ph,0} = \beta\left[M_{k,v}^* f_k^* \exp\left(-\frac{k^2}{4\lambda^2}\right) + M_{k,v} f_k \exp\left(-\frac{k^2}{4\lambda^2}\right)\right], \tag{14}$$

$$E_{r,0} = -\frac{2\pi g}{A}\sum_k \frac{1}{k}\exp\left(-\frac{k^2}{4\lambda^2}\right). \tag{15}$$

One can thus write the ground-state eigenenergy value, E_0, of the entire system as

$$E_0 = \beta\sum_{k,v}\left[V_F\hbar k f_k^* f_k + \hbar\omega_{so,v} f_k^* f_k + M_{k,v}^* f_k^* \exp\left(-\frac{k^2}{4\lambda^2}\right) + M_{k,v} f_k \exp\left(-\frac{k^2}{4\lambda^2}\right) - \frac{2\pi g}{A}\frac{1}{k}\exp\left(-\frac{k^2}{4\lambda^2}\right)\right], \tag{16}$$

where f_k^* and f_k are the variational parameters. From equation (16), one can use the variation method to obtain the ground-state energy of weakly coupled bound magnetopolarons in MG:

$$E_0 = \pm\left[\int_0^{k_c} \frac{Q^2\eta\hbar\omega_{so,v}\cdot e^{-2kz}}{4\pi\varepsilon_0\left(V_F\hbar k + \hbar\omega_{so,v}\right)} + \frac{2\pi g}{A}\frac{1}{k}\exp\left(-\frac{k^2}{4\lambda^2}\right)\mathrm{d}k\right], \tag{17}$$

where d represents the distance z between the substrate and the graphene monolayer and k_c is the cutoff wave number.

3. Results and Discussion

Three polar materials SiC, HfO_2, and $h-BN$ were selected as substrates for numerical calculation to analyse the effects of distance z, between graphene and substrates, the binding parameters g, magnetic field intensity B, and cutoff wave number k_c of phonons on the ground-state energy of the weakly coupled bound magnetopolarons in MG. Table 1 details the substrate parameters used for the calculations.

Figures 2 and 3 show the relationship between magnetic field strength and cutoff wave number in MG when $z = 1$nm and $g = 0.2$ for the three substrates. One can clearly observe that the original zero-Landau energy level is split into two

Table 1: Experimental parameters used in the numerical calculations.

Quantity (units)	SiC	HfO_2	$h-BN$
$k_0\,(\varepsilon_0)$	9.7	22.0	5.1
$k_\infty\,(\varepsilon_0)$	6.5	5.0	4.1
$\hbar\omega_{so,1}$ (meV)	116	19	101
$\hbar\omega_{so,2}$ (meV)	167	53	195

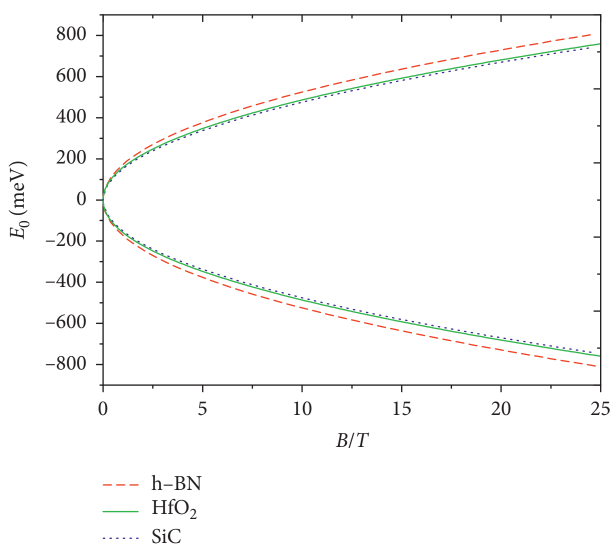

Figure 2: Variable magnetic field B versus the ground energy E_0.

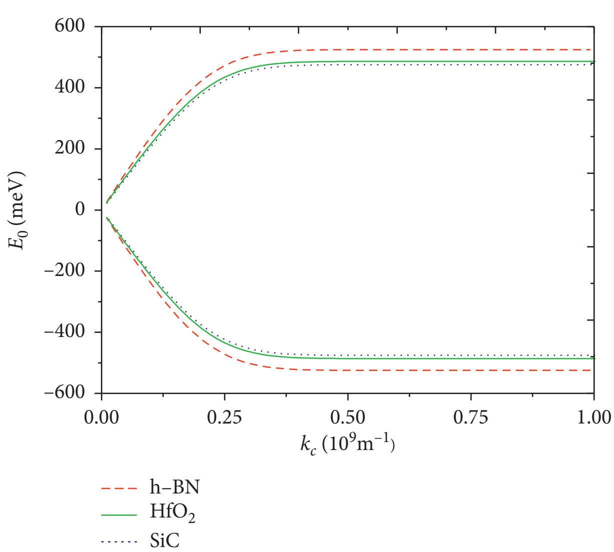

Figure 3: Variable cutoff wavenumber k_c versus the ground energy E_0.

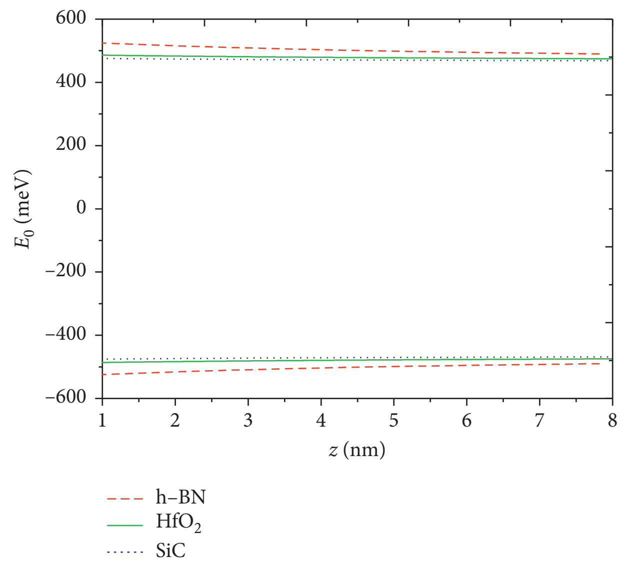

Figure 4: Variable substrate distance z versus the ground energy E_0.

symmetric energy bands. The splitting is the result of the well-known Lorenz effect and polaron effect. Additionally, it is trivial to see that the substrate material has an effect on the energy level value and that the absolute value of energy increases with increasing magnetic field strength and cutoff wavenumber. One notable difference is the apparent levelling off of ground-state energy once a threshold cutoff wavenumber is reached. The magnetic field can cause the splitting degree of ground-state energy, which is consistent with the results of references [5, 18, 20, 21]. We also calculated the effect of substrate material on the ground-state energy of graphene polaron. The greater dielectric constant of the substrate material can cause the stronger splitting of the two branches of the ground-state energy of the polaron. This is very important for the study of the surface optical polaron of the graphene on the substrate and also provides a theoretical reference for the experiment.

Figures 4 and 5 show the dependence of the ground-state energy of the weakly coupled bound magnetopolarons on the substrate distance z and Coulomb bound potential parameters. Figure 4 reveals that the absolute value of the ground-state energy decreases gradually as the substrate spacing increases, although only by ~50 meV over 8 nm. From equation (17), it is straightforward to see that the interaction between electrons on the graphene surface and phonons on the substrate surface is weakened with increased spacing. As can be seen from Figure 4, the band near the Dirac point splits into two opposing bands with linearly increasing absolute energy E_0. At constant distance z and cutoff wave number k_c, the enhancement of g increases the Coulomb binding energy and thereby increases the absolute energy of the ground state. This phenomenon is in agreement with the results of Ref. [9–11, 25]. However, we find that the parameter of Coulomb potential is an important factor in adjusting the polaron ground energy and causing the increase in splitting of energy level.

4. Conclusion

The ground-state energy of bound magnetopolarons in a single layer of graphene is calculated using the linear combination operators and LLP variational method, in the context of weakly coupling of electron and surface optical

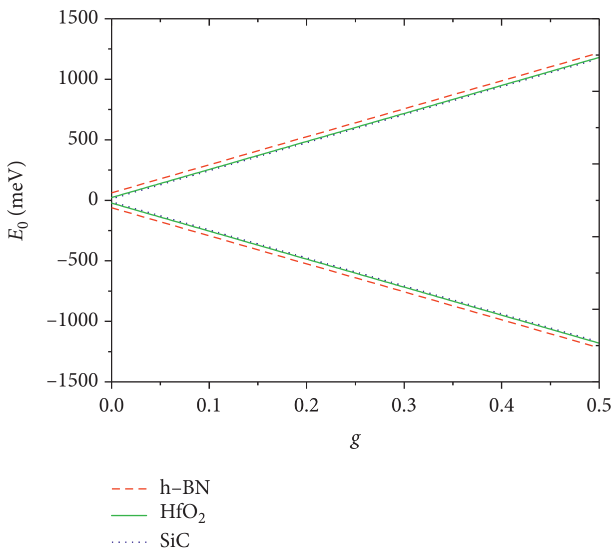

FIGURE 5: Variable parameter of Coulomb potential g versus the ground energy E_0.

(SO) phonon. The results show that the absolute value of the ground-state energy decreases when the magnetic field strength, bound potential strength, or cutoff wave number are increased. On the other hand, when one increases the distance between the graphene monolayer and substrate, the strength of the interaction decreases and the value of the ground-state energy is reduced. These results provide new ideas and methods for further understanding polaron effects in graphene and provide [25] theoretical basis for the preparation of functional quantum optical devices based on graphene structures.

Data Availability

No data were used to support this study.

Conflicts of Interest

The authors declare that they have no conflicts of interest.

Acknowledgments

This work was supported by the Natural Science Foundation of China (no. 11464033) and Natural Science Foundation of Inner Mongolia Autonomous Region of China (Grant no. 2019MS01008).

References

[1] A. H. Castro Neto, F. Guinea, N. M. R. Peres, K. S. Novoselov, and A. K. Geim, "The electronic properties of graphene," *Reviews of Modern Physics*, vol. 81, no. 1, pp. 109–162, 2009.

[2] K. S. Geim, "Nobel lecture: graphene: materials in the flatland," *Reviews of Modern Physics*, vol. 83, no. 3, pp. 837–849, 2011.

[3] H. Savin, P. Kuivalainen, S. Novikov, and N. Lebedeva, "Magnetic polaron formation in graphene-based single-electron transistor," *Physica Status Solidi B*, vol. 251, no. 4, pp. 864–870, 2014.

[4] V. M. Stojanović, V. Nenad, and C. Bruder, "Polaronic signatures and spectral properties of graphene antidot lattices," *Physical Review B*, vol. 82, p. 165410, 2010.

[5] B. S. Kandemir, "Possible formation of chiral polarons in graphene," *Journal of Physics: Condensed Matter*, vol. 25, no. 2, Article ID 025302, 2013.

[6] L. A. Ribeiro, F. F. Monteiro, W. F. da Cunha, and G. M. e Silva, "Charge carrier scattering in polymers: a new neutral coupled soliton channel," *Scientific Reports*, vol. 8, p. 1, 2018.

[7] C. Y. Chen, J. Avila, S. Wang et al., "Emergence of interfacial polarons from electron–phonon coupling in graphene/h-BN van der waals heterostructures," *Nano Letters*, vol. 18, p. 1082, 2018.

[8] R. Khordad and H. R. Rastegar Sedehi, "Study of non-extensive entropy of bound polaron in monolayer graphene," *Indian Journal of Physics*, vol. 92, no. 8, pp. 979–984, 2018.

[9] S. V. Kryuchkov and E. I. Kukhar, "Phonon-induced renormalization of the electron spectrum of biased bilayer graphene," *Superlattices and Microstructures*, vol. 117, pp. 288–292, 2018.

[10] C.-H. Jia, Z.-H. Ding, and J.-L. Xiao, "Gate-tunabe gap of heated monolayer graphene on substrates," *Physica B: Condensed Matter*, vol. 576, Article ID 411736, 2020.

[11] W.-P. Li, Z.-W. Wang, J.-W. YIN, and Y.-F. Yu, "The effects of the magnetopolaron on the energy gap opening in graphene," *Journal of Physics: Condensed Matter*, vol. 24, no. 13, Article ID 135301, 2012.

[12] H. T. Yang and W. H. Ji, "The effect of deformation potential magnetopolaron in graphene," *Journal of Low Temperature Physics*, vol. 179, no. 5-6, 2015.

[13] Y. Zhao, Z. P. Caddeng, Z. Jiang et al., "Symmetry breaking in the zero-energy landau level in bilayer graphene," *Physical Review Letters*, vol. 104, no. 6, Article ID 066801, 2010.

[14] Y. Xiao, W.-P. Li, Z.-Q. Li, and Z.-W. Wang, "Coulomb impurity effects on the zero-Landau level splitting of graphene on polar substrates," *Superlattices and Microstructures*, vol. 104, pp. 178–185, 2017.

[15] J. Zhu, S. M. Badayan, and F. M. Peeters, "Plasmonic excitations in Coulomb-coupledN-layer graphene structures," *Physical Review B*, vol. 87, no. 8, Article ID 085401, 2013.

[16] E. A. Hengrisen, Z. P. Cadden, Z. Jiang et al., "Interaction-induced shift of the cyclotron resonance of graphene using infrared spectroscopy," *Physical Review Letters*, vol. 104, Article ID 067404, 2010.

[17] Z.-W. Wang and S.-S. Li, "Lattice relaxation of graphene under high magnetic field," *Journal of Physics: Condensed Matter*, vol. 24, no. 26, Article ID 265302, 2012.

[18] Z. W. Wang, L. Liu, and Z. Li, "Gate-modulated weak anti-localization and carrier trapping in individual Bi2Se3 nanoribbons," *Applied Physics Letters*, vol. 106, no. 6, Article ID 1016011, 2015.

[19] Y. Sun, Z. H. Ding, and J. L. Xiao, "Temperature effect on the ground state energy and the longitudinal optical-phonon mean number of the impurity polaron in asymmetrical 2D RbCl semi-exponential quantum wells," *Materials Express*, vol. 9, pp. 371–375, 2019.

[20] Z.-H. Ding, Y.-B. Gen, C.-H. Jia, and J.-L. Xiao, "Temperature effect on the first excited state energy and average phonon number of bound magnetopolarons in monolayer graphene," *Journal of Electronic Materials*, vol. 48, no. 8, pp. 4997–5002, 2019.

[21] Z.-H. Ding, Y. Zhao, and J.-L. Xiao, "The first excited state energy of strong coupled bound polaron in monolayer graphene," *Superlattices and Microstructures*, vol. 113, pp. 20–24, 2018.

[22] Z.-H. Ding, Y. Zhao, and J.-L. Xiao, "The properties of strong couple bound polaron in monolayer graphene," *Superlattices and Microstructures*, vol. 97, pp. 298–302, 2016.

[23] Z.-H. Ding, Y. Zhao, and J.-L. Xiao, "The magnetic effect of polaron in monolayer graphene," *Journal of Low Temperature Physics*, vol. 182, no. 5-6, pp. 162–169, 2016.

[24] X.-J. Ma, C.-H. Jia, Z.-H. Ding, Y. Sun, and J.-L. Xiao, "Temperature effect of the bound magnetopolaron on the bandgap in monolayer graphene," *Superlattices and Microstructures*, vol. 123, pp. 30–36, 2018.

[25] W. J. Huybrechts, "Internal excited state of the optical polaron," *Journal of Physics C: Solid State Physics*, vol. 10, no. 19, pp. 3761–3768, 1977.